REPORT DOCUMENTATION PAGE

Form Approved
OMB No. 0704-0188

AD-A263 130

2. REPORT DATE	3. REPORT TYPE AND DATES COVERED
19 March 1993	Technical

4. TITLE AND SUBTITLE
Scanning Probe Lithography. 1. Scanning Tunneling Microscope-Induced Lithography of Self-Assembled *n*-Alkanethiol Monolayer Resists

5. FUNDING NUMBERS
N00014-91-1991

6. AUTHOR(S)
Claudia B. Ross, Li Sun, and Richard M. Crooks

7. PERFORMING ORGANIZATION NAME(S) AND ADDRESS(ES)
Department of Chemistry
University of New Mexico
Albuquerque, NM 87131

8. PERFORMING ORGANIZATION REPORT NUMBER
5

9. SPONSORING/MONITORING AGENCY NAME(S) AND ADDRESS(ES)
Office of Naval Research
800 North Quincy Street
Arlington, VA 22217-5000

10. SPONSORING/MONITORING AGENCY REPORT NUMBER

11. SUPPLEMENTARY NOTES
Prepared for Publication in *Langmuir*

12a. DISTRIBUTION/AVAILABILITY STATEMENT
This document has been approved for public release and sale; its distribution is unlimited

12b. DISTRIBUTION CODE
N00179

13. ABSTRACT (*Maximum 200 words*)

The tip of a scanning tunneling microscope was used to fabricate geometrically well-defined structures within organized, self-assembled monolayer resists that have critical dimensions ranging from 60 nm to 5 μm. To achieve nanometer-scale lithography, a Au(111) substrate was coated with a self-assembled monolayer of $HS(CH_2)_{17}CH_3$, which functions as an ultrathin (~2.5 nm) resist, and then the resist was etched by an STM tip. This treatment results in window-like features that penetrate the organic monolayer. Nanolithographically defined features have been characterized by scanning tunneling microscopy, scanning electron microscopy, and electrochemical methods. For example, since mass and electron transfer to the conductive Au substrate are blocked by the monolayer everywhere except in the STM-etched regions, the windows serve as ultramicroelectrodes. The limiting current that results from radial diffusion of a bulk-phase redox species to the etched window is in close agreement with that predicted by theory.

14. SUBJECT TERMS	15. NUMBER OF PAGES
	16. PRICE CODE

17. SECURITY CLASSIFICATION OF REPORT	18. SECURITY CLASSIFICATION OF THIS PAGE	19. SECURITY CLASSIFICATION OF ABSTRACT	20. LIMITATION OF ABSTRACT
Unclassified	Unclassified	Unclassified	

OFFICE OF NAVAL RESEARCH

GRANT N00014-91-J-1991

R&T Code s400x084yi01

Technical Report No. 5

Scanning Probe Lithography. 1. Scanning Tunneling Microscope-Induced Lithography of Self-Assembled *n*-Alkanethiol Monolayer Resists

by

Claudia B. Ross, Li Sun, and Richard M. Crooks

Prepared for Publication

in

Langmuir

Department of Chemistry
University of New Mexico
Albuquerque, NM 87131

March 19, 1993

Technical Report 5.

Scanning Probe Lithography. 1. Scanning Tunneling Microscope-Induced Lithography of Self-Assembled *n*-Alkanethiol Monolayer Resists

Claudia B. Ross, Li Sun, and Richard M. Crooks*

Prepared for publication in *Langmuir*

Abstract

The tip of a scanning tunneling microscope was used to fabricate geometrically well-defined structures within organized, self-assembled monolayer resists that have critical dimensions ranging from 60 nm to 5 μm. To achieve nanometer-scale lithography, a Au(111) substrate was coated with a self-assembled monolayer of $HS(CH_2)_{17}CH_3$, which functions as an ultrathin (~2.5 nm) resist, and then the resist was etched by an STM tip. This treatment results in window-like features that penetrate the organic monolayer. Nanolithographically defined features have been characterized by scanning tunneling microscopy, scanning electron microscopy, and electrochemical methods. For example, since mass and electron transfer to the conductive Au substrate are blocked by the monolayer everywhere except in the STM-etched regions, the windows serve as ultramicroelectrodes. The limiting current that results from radial diffusion of a bulk-phase redox species to the etched window is in close agreement with that predicted by theory.

SUMMARY

The tip of a scanning tunneling microscope was used to fabricate geometrically well-defined structures within organized, self-assembled monolayer resists that have critical dimensions ranging from 60 nm to 5 μm. To achieve nanometer-scale lithography, a Au(111) substrate was coated with a self-assembled monolayer of $HS(CH_2)_{17}CH_3$, which functions as an ultrathin (~2.5 nm) resist, and then the resist was etched by an STM tip. This treatment results in window-like features that penetrate the organic monolayer. Nanolithographically defined features have been characterized by scanning tunneling microscopy, scanning electron microscopy, and electrochemical methods. For example, since mass and electron transfer to the conductive Au substrate are blocked by the monolayer everywhere except in the STM-etched regions, the windows serve as ultramicroelectrodes. The limiting current that results from radial diffusion of a bulk-phase redox species to the etched window is in close agreement with that predicted by theory.

INTRODUCTION

We wish to report the first examples of scanning probe-induced lithography of organized monolayer resists.[1] In this experiment, resists consist of monolayers of self-assembled *n*-alkanethiols which, when confined to Au(111) substrates, form approximately 2.5 nm-thick barriers to mass and electron transfer.[2-4] When a scanning tunneling microscope (STM) tip is positioned near the Au substrate and rastered across the surface, it induces desorption of the monolayer resist. Results obtained by STM, electrochemical methods, and scanning electron microscopy confirm that this technique is useful for fabricating geometrically well-defined, nanometer-scale structures such as ultramicroelectrodes.

Most lithographic processes rely on light-induced chemical transformations of organic polymers for fabrication of micron-scale surface features. Present commercial photolithographic processes are wavelength-limited to about 0.5 μm critical dimensions,[5] but the development of new technologies that can reduce this limit to 0.1 - 0.2 μm is essential for high-density, high-speed microelectronic applications. The present state-of-the-art for lithographically-defined surface features is quantum dot cylinders with diameters of about 100 nm and thicknesses around 10 nm.[6] The thickness is limited by the quality of molecular beam epitaxy-deposited thin films, and the lateral dimension is defined by the resolution of electron beam lithography. In principle, electron beam lithography should only

be limited by the wavelength of an electron, about 0.02-0.05 nm, however, as a result of forward scattering of electrons in the resist and backscattering from the substrate, features with critical dimensions less than 100 nm may not be attainable. Because of the physical limitations of present technologies, we feel it is desirable to evaluate alternative approaches for fabricating structures with critical dimensions in the range of 5-200 nm.

Scanning probe devices were first developed by Binnig et al. in 1982,[7] and since that time have been used primarily as tools for obtaining topographical and electronic surface maps. However, they can also be used to directly modify the chemical or physical structure of surfaces.[8] In this paper, we present the first example of deliberate STM etching of an organic monolayer resist to produce well-defined features with critical dimensions as small as 60 nm.[9] Since it has been clearly demonstrated that interpretation of STM images is sometimes ambiguous,[10] we also provide an independent electrochemical analysis of some of the larger lithographically-defined features.

EXPERIMENTAL SECTION

Substrate Preparation. A 0.25 mm-diameter Au wire (99.998%) was cleaned by dipping in freshly prepared "piranha solution" (3:1 conc. H_2SO_4:30% H_2O_2, **Caution:** piranha solution reacts violently with organic compounds, and it should not be stored in closed

containers). Au(111) surfaces were prepared by melting the wire in a H_2/O_2 flame under N_2, and then annealing in a cooler region of the flame.[11-13] This treatment results in approximately 1 mm-diameter spheres that contain a few Au(111) facets on the surface. The facets are typically elliptical, with a long axis of about 100 μm, and are composed of atomically flat terraces about 100 nm wide. The Au balls were cleaned again in piranha solution and then rinsed with ethanol. To facilitate electrochemical experiments, the entire ball, with the exception of a single Au(111) facet, was covered with silicone rubber (Dow-Corning, Catalog No. 698). Prior to monolayer adsorption, the exposed facet was usually polished electrochemically in an aqueous 0.1 M $HClO_4/5x10^{-5}$ M HCl solution: this process eliminates adsorbed organic material from the Au surface and tends to reduce the number of Au surface defects.[13,14] Cyclic voltammetry confirmed the presence of a clean Au(111) surface. The freshly prepared surface was immersed in a 1 mM ethanolic solution of octadecylmercaptan, $HS(CH_2)_{17}CH_3$, for 24 h, removed, rinsed, and then attached to a home-built STM-substrate holder for subsequent etching and analysis.

Scanning Tunneling Microscope Etching and Imaging. A Nanoscope II STM (Digital Instruments, Santa Barbara, CA) was used for all STM experiments. Images were obtained using a bias voltage of +300 mV and tip currents in the range 0.10 to 0.11 nA (scan rate = 1.34 Hz). Positive bias voltages indicate that electrons tunnel from the STM tip to the Au substrate. Tips were mechanically cut from

Pt/Ir (80/20%) wire. The etching conditions depended on the size of the nanolithographically-defined feature, and they are discussed in the text. The STM *z*-piezo was calibrated by measuring several independently prepared Au(111) monoatomic step edges and correlating the mean experimental value to the theoretical Au(111) interlayer spacing of 0.235 nm.

Electrochemistry. Electrochemical experiments were carried out in a single-compartment, three-electrode, glass cell containing a Ag/AgCl, KCl(sat'd) reference electrode and a Pt counter electrode. Cyclic voltammograms were obtained in purified (Milli-Q, Millipore), deoxygenated aqueous solutions consisting of 5 mM $Ru(NH_3)_6^{3+}$ and 0.1 M KCl.

RESULTS AND DISCUSSION

STM images of a stepped Au(111) surface covered with a single monolayer of $HS(CH_2)_{17}CH_3$ before and after intentional probe etching are shown in Figure 1. The top 400 x 400 nm image was

Figure 1

obtained with a +300 mV bias voltage and a tunneling current of 0.10 nA. The Au surface contains primarily 100-300-nm-wide atomically flat terraces separated by monoatomic steps. Small circular defect structures, typically 5 nm in diameter, always

appear homogeneously distributed within the $HS(CH_2)_{15}CH_3$ monolayer.[9b,13] We are studying these structures, but at the present time we are uncertain of their precise structure or origin. Immediately after obtaining the top image, the center 100 x 100 nm region was scanned four times using the same mild conditions used to obtain the top image. High resolution images of this region, which are not shown here, indicate that the small defect structures shown in the top image enlarge and eventually grow together to form much larger defects as a result of tip-substrate interactions. The bottom part of Figure 1 shows a second image of the same region after imaging the center part four times. Three aspects of the bottom micrograph are worth noting. First, the center-most region of the organic surface has been etched by the STM tip. Second, there is evidence that the organic material removed from the center part of the scan has been deposited on the left and right edges of the etched feature. Third, the small defects surrounding the etched portion of the surface have been enlarged somewhat even though they have only been exposed to the tip during two scans. These data clearly demonstrate the feasibility of using tip-substrate interactions to create high-resolution, nanometer-scale features on surfaces.

The physical basis for STM-tip-induced lithography is not certain at the present time, but some combination of the following four phenomena seems likely to contribute: (1) electron-beam-induced degradation or desorption; (2) field ionization of molecules resident near the tip-substrate gap that are accelerated towards the surface, thereby desorbing the resist; (3) physical

abrasion of the Au surface by the tip; (4) Joule heating of the substrate, arising from current flowing through the gap resistance, and subsequent thermal desorption of the resist. The fundamental problem associated with assigning the particular tip-substrate interaction(s) responsible for monolayer removal arises from the uncertain *z*-axis displacement of the tip relative to the substrate during imaging. Data discussed later suggest the tip might be 1-2 nm above the Au surface during imaging, but since STM images are a convolution of tunneling probability and topography, this estimate is quite speculative. Moreover, since each STM scan removes some of the organic material from the surface, it is likely that *z*-displacement is also a function of the number of times the surface is scanned and, of course, the bias voltage and tunneling current employed. Based on the data shown in Figure 1, particularly the distribution of organic material in the bottom image, our present hypothesis focuses on physical abrasion of the surface as the dominant tip-substrate interaction responsible for STM-induced nanolithography *under the conditions employed in these experiments*.

Figure 2A shows three 60 nm x 60 nm STM-defined features

Figure 2

confined to a single Au(111) terrace. In contrast to the incomplete etching of the structure shown in Figure 1, all of the organic material appears to have been removed within these etched regions. This results from the more vigorous etching conditions

used to fabricate the structures shown in Figure 2A: four scans with the tip biased at +3 V and a tip current of 3.11 nA (scan rate = 31.25 Hz) followed by four scans at +300 mV and the same current and scan rate. The first set of scans apparently removes most of the monolayer resist, but the second set is necessary to completely remove the organic material from the bottom of the etched features. We have been able to create geometrically well-defined structures similar to those shown in Figure 2 that are as small as 25 x 25 nm, and it appears that the limit of resolution is determined only by the size of the tip and the diameter of the resist molecules. Such structures are dimensionally stable for at least several days.

Line scans corresponding to the data in Figure 2A are shown in Figure 2B. We intentionally scanned over an atomic step as an internal calibration of topography in acquiring these data. This feature can be seen in line scans 1-3, and it clearly indicates that the morphology of the underlying Au substrate can be reliably imaged through the organic monolayer: the line scans indicate that the Au step height is 0.22 nm, which is close to the 0.24 nm interlayer spacing of Au(111).[12]

The most interesting aspect of the line scans relates to the "depth" of the etched features. FTIR and ellipsometric data indicate the height of $HS(CH_2)_{17}CH_3$ monolayers range from about 2.2 nm to about 2.8 nm, but the line scans shown in Figure 2B reproducibly indicate a depth of only 0.7±0.1 nm.[2-4] Electrochemical data discussed later strongly suggest, but do not unambiguously prove, that most of the organic resist material has

been removed from the bottom of the etched features. If the bottoms of the pits are clean, and if the Au itself has not been etched, the STM tip is probably within, rather than above, the n-alkanethiol monolayer during imaging. Kim and Bard reported the depth of somewhat smaller STM-induced defects to be 0.8±0.1 nm, and they explained this anomalous behavior as resulting from differences in tunneling probabilities.[9b] While our data support these previous results, we do not believe it is possible to confirm either model at the present time.

Since it has been well-established that STM images of organic surfaces are difficult to unambiguously interpret,[10] we used electrochemical methods to confirm the STM data. Additionally, the data presented here clearly indicate that STM lithography is a good means for fabricating ultramicroelectrodes. The electrochemical experiment is illustrated in Scheme I, and the

Scheme I

details of electrode fabrication were discussed in the experimental section.

Figure 3A is the cyclic voltammetric response to a 5 mM

Figure 3

$Ru(NH_3)_6^{3+}$ solution obtained for a Au(111) facet after masking with silicone rubber, but prior to $HS(CH_2)_{17}CH_3$ modification. The data are intermediate between those expected for linear and radial diffusion: a consequence of the small size of the Au(111) facet.

After monolayer modification, Figure 3B indicates that the Faradaic current is significantly reduced and consists of a combination of Faradaic leakage current that occurs at adventitious defects in the monolayer, as indicated in Scheme 1 and tunneling current through the monolayer to bulk phase $Ru(NH_3)_6^{3+}$. The cyclic voltammetry shown in Figure 3C results after STM tip-induced etching of one 5 x 5 μm window within the $HS(CH_2)_{17}CH_3$ monolayer resist. A scanning electron micrograph of such a window is shown in Figure 4. These large features were

Figure 4

fabricated by scanning the surface twice with a bias voltage of +0.5 V, a tunneling current of 0.11 nA, and a scan rate of 1.34 Hz. The sigmoidal shape of the voltammogram is characteristic of radial diffusion to a small electrode, in this case the STM-etched ultramicroelectrode. We can use eq 1 to calculate a theoretical value for the limiting voltammetric current, i_l, if we model the electrode as a disk of radius r, rather than as a square.[15]

$$i_l = 4nFDCr \qquad (1)$$

For this experiment, n = 1 equiv/mol, F = 96485 C/equiv, D = 7.1 x 10^{-6} cm^2/s,[16] and C = 5.0 x 10^{-6} mol/cm^3. Approximating i_l by subtracting the residual current at -0.38 V in Figure 3B from the current in Figure 3C, we calculate a value of r = 3.6 μm. We believe the difference between this value and the one obtained by

visual inspection of Figure 4, about 0.5 μm, arises primarily from our assumption concerning the shape of the electrode; however, the main point is that, to a first approximation, the electrochemical data confirm the STM results.

After obtaining the voltammetry shown in Figure 3C, we etched three additional 5 x 5 μm windows in the organic thin layer resist in the configuration illustrated in Figure 3D. This process results in an array of ultramicroelectrodes and a limiting current about three times larger than that shown in Figure 3C. We expected the limiting current to be four times larger, but since the four electrodes are so closely spaced, their diffusion layers overlap.[15]

A plot of E versus $\log[(i_l-i)/i]$ for potentials on the rising part of the voltammograms shown in Figures 3C and 3D yields a slope of 90 mV, close to the value for a thermodynamically reversible one-electron transfer reaction of 59 mV.[15] This result supports, but does not unambiguously confirm, our contention that most of the organic material has been removed from the electrode surface in the etched areas, since a significant insulating layer would further reduce the rate of electron transfer between the electrode and $Ru(NH_3)_6^{3+}$, and thus decrease the slope of the rising part of the cyclic voltammogram. Figure 4 suggests the presence of some organic material within etched region, but the distribution is such that the effect on the electrochemical response should be negligible. The three important points that result from the data shown in Figures 3 and 4 are: (1) it is possible to use the STM tip to nanolithographically define

electrode arrays; (2) additional lithographically-defined features result in additional Faradaic current of the correct magnitude; (3) since the electron transfer kinetics are facile, most organic material has been removed from the Au surface in the vicinity of the etched features.

CONCLUSIONS

This preliminary report provides the first example of intentional STM fabrication of well-defined features within a self-assembled monolayer resist. The essential features of the STM images of the nanolithographically-defined windows are confirmed by companion electrochemical experiments and scanning electron micrographs. Combination of the three methods yields complementary information about the nature of the patterns, and it also provides a new means for studying the nature of the tip-monolayer interaction. Perhaps the most important aspect of this work is that the monolayer resists are sufficiently thin to permit electron tunneling, but sufficiently thick to effectively block significant mass transfer and Faradaic electron transfer across them.

At the present time, we are pursuing several aspects of the preliminary data presented here. First, we are using low temperature chemical vapor deposition techniques to selectively metallize etched regions.[17] Second, we are trying to improve the blocking quality of the monolayers so that we can construct very well-defined ultramicroelectrodes in the size range 1-10 nm; at

the present time electrodes with a critical dimension less than 100 nm are too leaky to be useful. Finally, we are just beginning experiments designed to elucidate the mechanism responsible for tip-induced lithography. Preliminary results from these experiments will be reported shortly.

ACKNOWLEDGMENTS

We gratefully acknowledge the Office of Naval Research for full support of this work.

REFERENCES

1. The results discussed here have previously been presented orally. (a) Crooks, R. M.; Sun, L.; Thomas, R.; Challapakul, O. *Abstracts of Papers*, 18th Annual Meeting of the Federation of Analytical Chemistry and Spectroscopy Societies, Anaheim, CA; Federation of Analytical Chemistry and Spectroscopy Societies: Leavenworth, KS, 1991; Abstract 657. (b) Crooks, R. M.; Ross, C. B.; Sun, L. *Abstracts of Papers*, 182nd National Meeting of the Electrochemical Society, Toronto, Canada, 1992; Abstract 629.
2. Nuzzo, R. G.; Allara, D. L. *J. Am. Chem. Soc.* **1983**, *105*, 4481.
3. Bain, C. D.; Troughton, E. B.; Tao, Y-T.; Evall, J.; Whitesides, G. M.; Nuzzo, R. G. *J. Am. Chem. Soc.* **1989**, *111*, 321 and references therein.
4. Dubois, L. H.; Nuzzo, R. G. *Annu. Rev. Phys. Chem.* **1992**, *43*, 437, and references therein.
5. Wolf, S.; Tauber, R. N. *Silicon Processing for the VLSI Era*; Lattice: Sunset Beach, CA, 1986; Chapter 14.
6. (a) Randall, J. N.; Reed, M. A.; Matyi, R. J.; Moore, T. M. *J. Vac. Sci. Technol. B.* **1988**, *6*, 1861. (b) Randall, J. N.; Reed, M. A.; Moore, T. M.; Matyi, R. J.; Lee, J. W. *J. Vac. Sci. Technol. B.* **1988**, *6*, 302.
7. Binnig, G.; Rohrer, H.; Gerber, Ch.; Weibel, E. *Phys. Rev. Lett.* **1982**, *49*, 57.
8. The following references are a brief but representative cross section of the scanning probe modification literature: (a)

Ringger, M.; Hidber, H. R.; Schlogl, R.; Oelhafen, P.; Güntherodt, H.-J. *Appl. Phys. Lett.* **1985**, *46*, 832. (b) Stauter, U.; Wiesendanger, R.; Eng, L.; Rosenthaler, L.; Hidber, H.-R.; Güntherodt, H.-J.; Garcia, N. *Appl. Phys. Lett.* **1987**, *51*, 244. (c) Lin, C. W.; Fan, F-R.; Bard, A. J. *J. Electrochem. Soc.* **1987**, *134*, 1038. (d) Foster, J. S.; Frommer, J. E.; Arnett, P. C. *Nature* **1988**, *331*, 324. (e) McCord, M. A.; Pease, R. F. W. *J. Vac. Sci. Technol. B* **1988**, *6*, 293. (f) McCord, M. A.; Kern, D. P; Chang, T. H. P. *J. Vac. Sci. Technol. B* **1988**, *6*, 1877. (g) Staufer, U.; Wiesendanger, R.; Eng, L.; Rosenthaler, L.; Hidber, H.-R.; Güntherodt, H.-J.; Garcia, N. *J. Vac. Sci. Technol. A* **1988**, *6*, 537. (h) Schneir, J.; Sonnenfeld, R.; Marti, O.; Hansma, P. K. *J. Appl. Phys.* **1988**, *63*, 717. (i) Craston, D. H.; Lin, C. W.; Bard, A. J. *J. Electrochem. Soc.* **1988**, *135*, 785. (j) Zhang, H.; Hordon, L. S.; Kuan, S. W. J.; Maccagno, P.; Pease, R. F. W. *J. Vac. Sci. Technol. B* **1989**, 7, 1717. (k) Garfunkel, E.; Rudd, G.; Novak, D.; Wang, S.; Ebert, G.; Greenblatt, M.; Gustafsson, T.; Garofalini, S. H. *Science* **1989**, *246*, 99. (l) Li, Y. Z.; Vazquez, L.; Piner, R.; Andres, R. P.; Reifenberger, R. *Appl. Phys. Lett.* **1989**, *54*, 1424. (m) Parkinson, B. *J. Am. Chem. Soc.* **1990**, *112*, 7498. (n) Lyo, I-W.; Avouris, P. *Science* **1991**, *253*, 173. (o) Whitman, L. J.; Stroscio, J. A.; Dragoset, R. A.; Celotta, R. J. *Science* **1991**, *251*, 1206. (p) Hansma, H. G.; Gould, S. A. C.; Hansma, P. K.; Gaub, H. E.; Longo, M. L.; Zasadzinski, J. A. N. *Langmuir* **1991**, *7*, 1051. (q) Hoh, J. H.; Lal, R.; John, S. A.; Revel, J.-P.; Arnsdorf, M. F. *Science* **1991**, *253*, 1405. (r) Goss, C. A.;

Brumfield, J. C.; Irene, E. A.; Murray, R. C. *Langmuir* **1992**, 8, 1459. (s) Brumfield, J. C.; Goss, C. A.; Irene, E. A.; Murray, R. C. *Langmuir* **1992**, *8*, 2810. (t) Abbott, N. L.; Folkers, J. P.; Whitesides, G. M. *Science* **1992**, *257*, 1380.

9. There have been two prior papers that are particularly relevant to the results described here: (a) Casillas et al. showed that an STM tip could be used to etch nanometer-scale features in a thin layer of Pt-confined TiO_2 (Casillas, N.; Snyder, S. R.; White, H. S. *J. Electrochem. Soc.* **1991**, *138*, 641). (b) Kim and Bard demonstrated that STM imaging of *n*-alkanethiol monolayers results in lateral expansion of adventitious defects (Kim, Y.-T.; Bard, A. J. *Langmuir* **1992**, *8*, 1096).
10. (a) Chang, H.; Bard, A. J. *Langmuir* **1991**, 7, 1143. (b) Clemmer, C. R.; Beebe, T. P., Jr. *Science* **1991**, *251*, 640.
11. Hsu, T.; Cowley, J. M. *Ultramicrosc.*, **1983**, *11*, 125.
12. Snyder, S. R. *J. Electrochem. Soc.* **1992**, *139*, 5C.
13. Sun, L.; Crooks, R. M. *J. Electrochem. Soc.* **1991**, *138*, L23.
14. Trevor, D. J.; Chidsey, C. E. D.; Loiacono, D. N. *Phys. Rev. Lett.* **1989**, *62*, 929.
15. Wightman, R. M.; Wipf, D. O. In *Electroanalytical Chemistry*, Bard, A. J., Ed.; Marcel Dekker: NY, 1989; Vol. 15, p. 267.
16. Licht, S.; Cammarata, V.; Wrighton, M. S. *J. Phys. Chem.* **1990**, *94*, 6133.
17. (a) Shin, H. K.; Chi, K. M.; Farkas, J.; Hampden-Smith, M. J.; Kodas, T. T.; Duesler, E. N. *Inorg. Chem.* **1992**, *31*, 424. (b) Shin, H. K.; Chi, K. M.; Hampden-Smith, M. J.; Kodas, T. T.; Farr, J. D.; Paffett, M. *Chem. Mater.* **1992**, *4*, 788.

FIGURE CAPTIONS

1. STM images of a Au(111) surface modified with a monolayer of $HS(CH_2)_{17}CH_3$. (Top) First 400 x 400 nm scan. (Bottom) Second 400 x 400 nm scan. Four scans of the center 100 x 100 nm region of the surface were obtained prior to recording of the bottom image. Conditions for all six scans: bias voltage = +300 mV; tunneling current = 0.10 nA; scan rate = 1.34 Hz.

2. (A) STM image of a Au(111) substrate modified with a monolayer of $HS(CH_2)_{17}CH_3$ after opening three 60 x 60 nm windows. STM etching conditions: four scans (bias voltage = +3 V; tunneling current = 0.11 nA; scan rate = 31.25 Hz) followed by four additional scans (bias voltage = +300 mV; tunneling current = 0.11 nA; scan rate = 31.25 Hz). (B) STM line scans through the etched regions which are shown in (A) and illustrated schematically to the right of the line scans. The vertical displacement (v.d.) between the arrows is indicated next to each line scan.

3. Electrochemical results obtained at (A) a naked Au(111) facet; (B) the same facet after modification with a monolayer of $HS(CH_2)_{17}CH_3$; (C) the same facet after STM fabrication of a single 5 x 5 μm ultramicroelectrode; (D) the same facet after fabricating four 5 x 5 μm ultramicroelectrodes spaced as indicated schematically to the left. Conditions: solution, 5 mM $Ru(NH_3)_6^{3+}$/0.1 M KCl; scan rate = 100 mV/s.

4. Scanning electron micrograph of a 5 x 5 μm (nominal), STM-defined ultramicroelectrode.

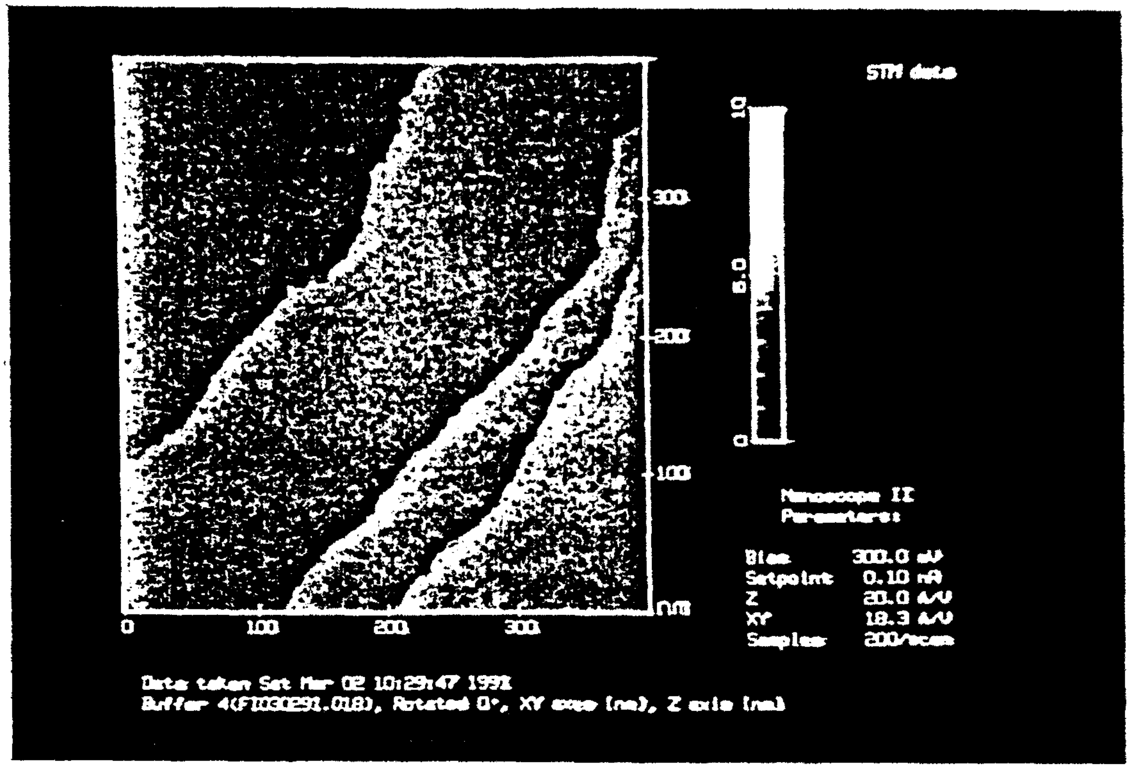
STM data
10
5.0
0
300
200
100
nm
0
100
200
300
Nanoscope II
Parameters:
Bias 300.0 mV
Setpoint 0.10 nA
Z 20.0 A/V
XY 18.3 A/V
Samples 200/scan
Data taken Sat Mar 02 10:29:47 1991
Buffer 4(FI030291.018), Rotated 0°, XY axes [nm], Z axis [nm]

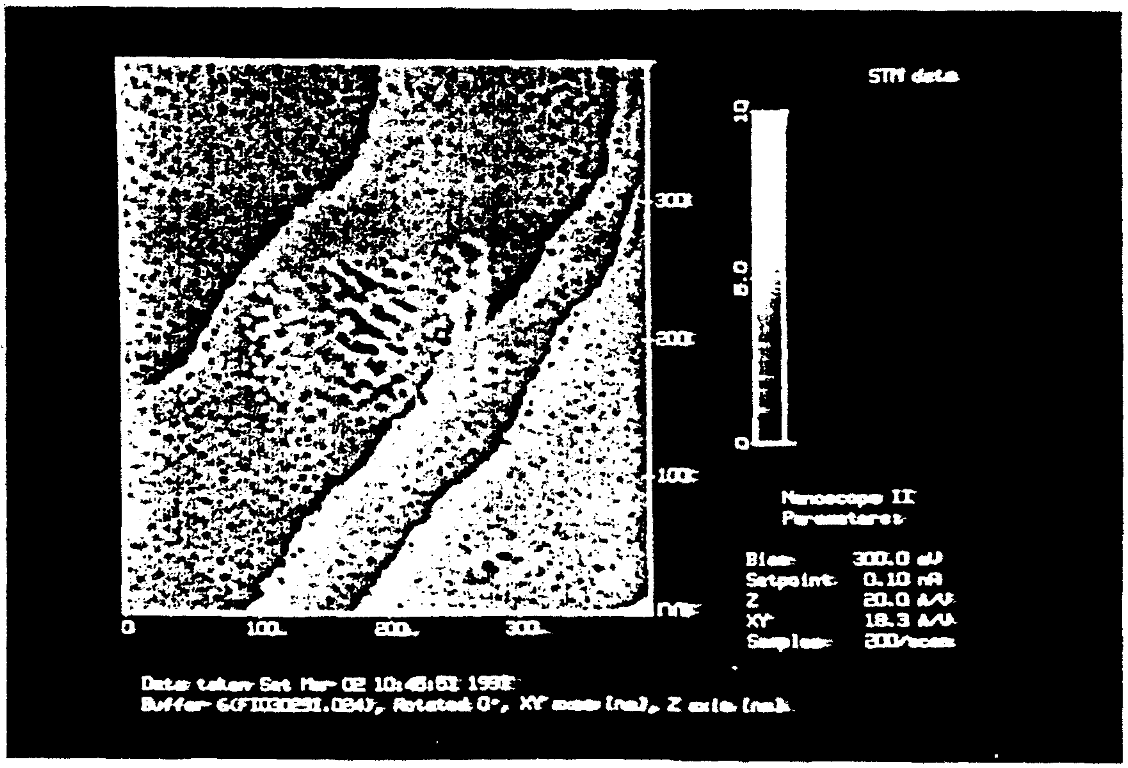
STM data
10
5.0
0
300
200
100
nm
0
100
200
300
Nanoscope II
Parameters:
Bias 300.0 mV
Setpoint 0.10 nA
Z 20.0 A/V
XY 18.3 A/V
Samples 200/scan
Data taken Sat Mar 02 10:45:51 1991
Buffer 6(FI030291.034), Rotated 0°, XY axes [nm], Z axis [nm]

A

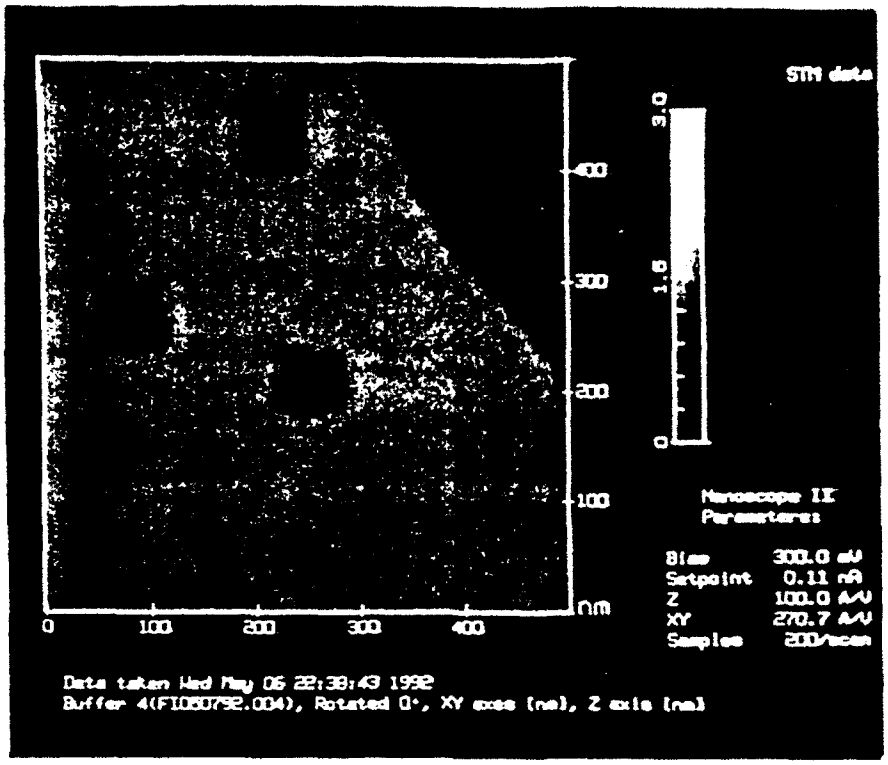

B

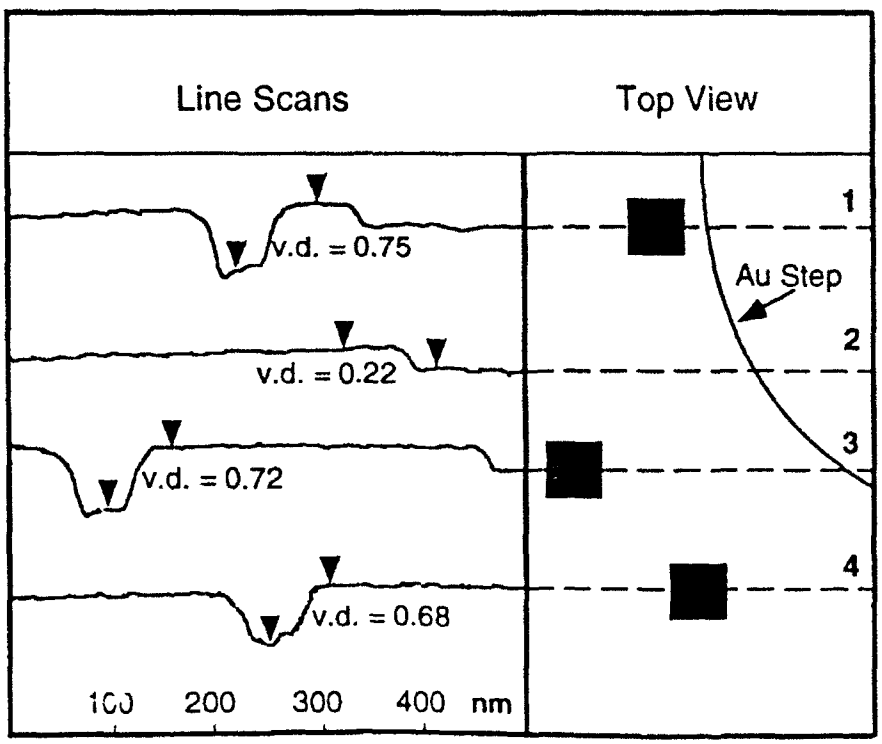

Figure 2/Ross et al.

Substrate Modification

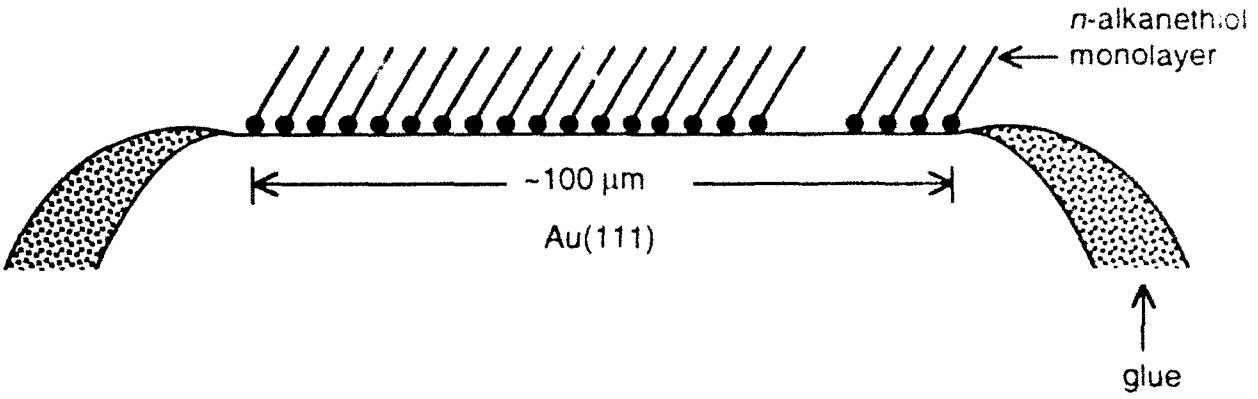

STM Lithography

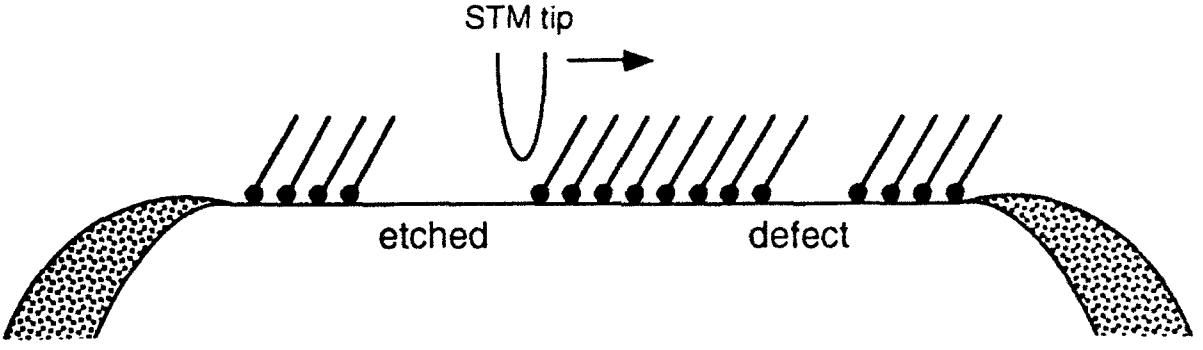

Electrochemical Analysis

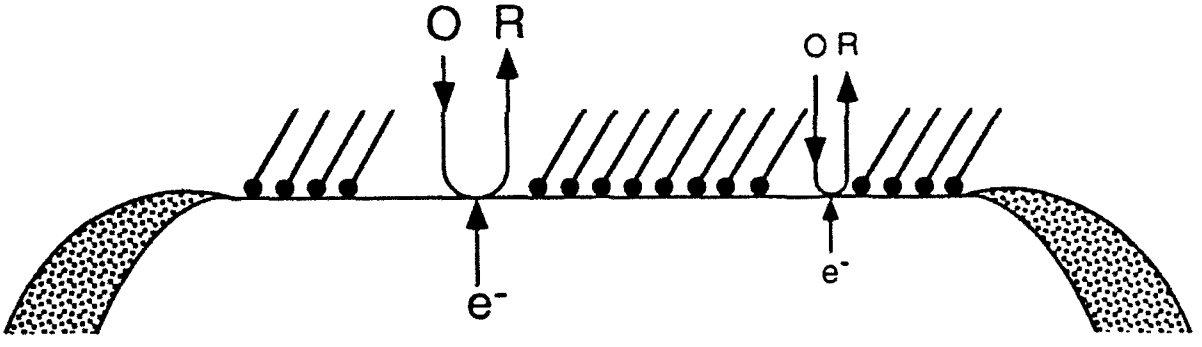

Scheme I - Ross et. al.

A. Naked Au (111) Facet

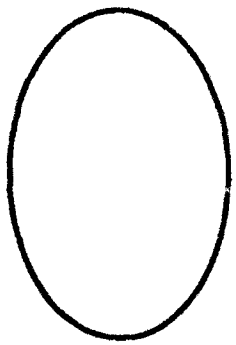

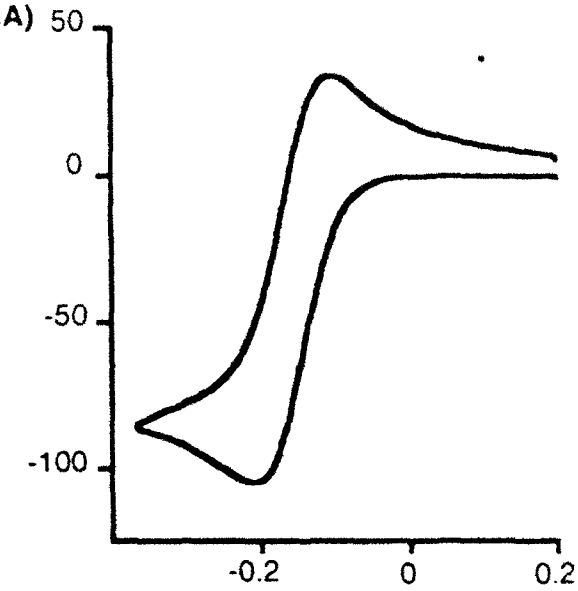

B. Au (111) / $HS(CH_2)_{17}CH_3$

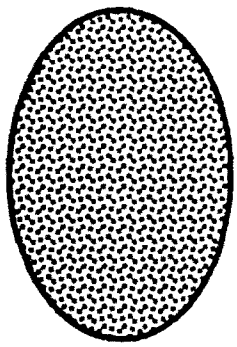

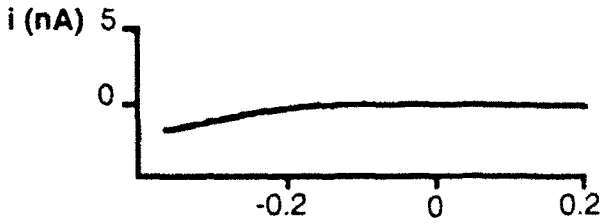

C. One 5 x 5 µm window

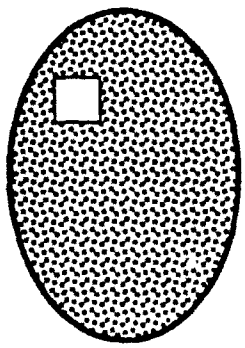

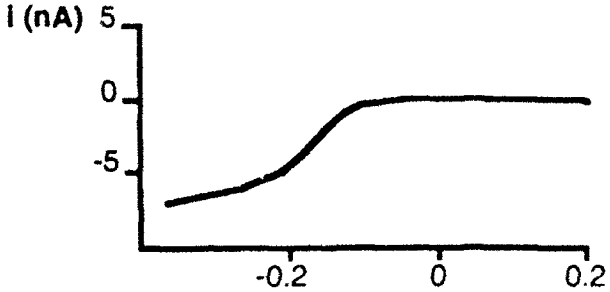

D. Four 5 x 5µm windows

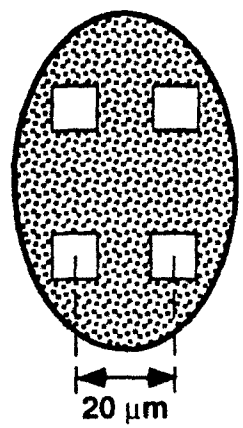

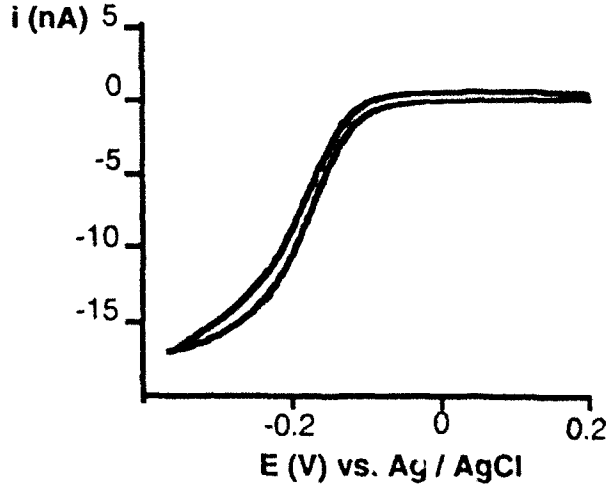

Figure 3/Ross et al.

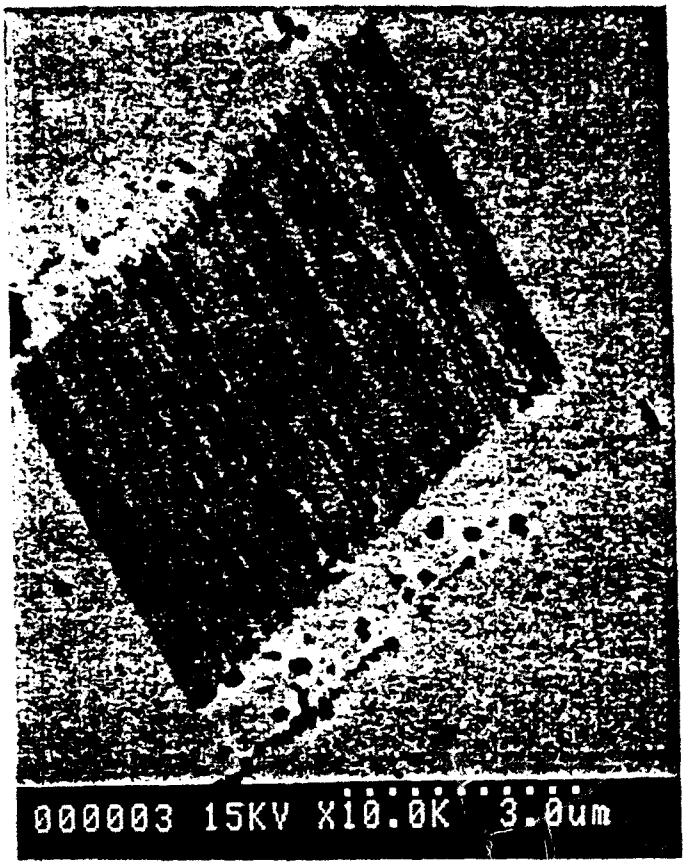

Fig. 4
Ross et al.

TECHNICAL REPORT DISTRIBUTION LIST - GENERAL

Office of Naval Research (2)*
Chemistry Division, Code 1113
800 North Quincy Street
Arlington, Virginia 22217-5000

Dr. James S. Murday (1)
Chemistry Division, Code 6100
Naval Research Laboratory
Washington, D.C. 20375-5000

Dr. Robert Green, Director (1)
Chemistry Division, Code 385
Naval Air Weapons Center
Weapons Division
China Lake, CA 93555-6001

Dr. Elek Lindner (1)
Naval Command, Control and Ocean
Surveillance Center
RDT&E Division
San Diego, CA 92152-5000

Dr. Bernard E. Douda (1)
Crane Division
Naval Surface Warfare Center
Crane, Indiana 47522-5000

Dr. Richard W. Drisko (1)
Naval Civil Engineering
Laboratory
Code L52
Port Hueneme, CA 93043

Dr. Harold H. Singerman (1)
Naval Surface Warfare Center
Carderock Division Detachment
Annapolis, MD 21402-1198

Dr. Eugene C. Fischer (1)
Code 2840
Naval Surface Warfare Center
Carderock Division Detachment
Annapolis, MD 21402-1198

Defense Technical Information
Center (2)
Building 5, Cameron Station
Alexandria, VA 22314

* Number of copies to forward